JOC The Journal of Organic Chemistry

Article

pubs.acs.org/joc

Synthesis of Perylene Imide Diones as Platforms for the Development of Pyrazine Based Organic Semiconductors

Paula de Echegaray,[†] María J. Mancheño,[†] Iratxe Arrechea-Marcos,[‡] Rafael Juárez,[§] Guzmán López-Espejo,[‡] J. Teodomiro López Navarrete,[‡] María Mar Ramos,[§] Carlos Seoane,[†] Rocío Ponce Ortiz,*[,‡] and José L. Segura*[,†]

[†]Departamento de Química Orgánica I, Facultad de Ciencias Químicas, Universidad Complutense de Madrid, 28040 Madrid, Spain

[‡]Departamento de Química Física, Facultad de Ciencias, Universidad de Málaga, 29071 Málaga, Spain

[§]Departamento de Tecnología Química y Ambiental, Universidad Rey Juan Carlos, Madrid 28933, Spain

Supporting Information

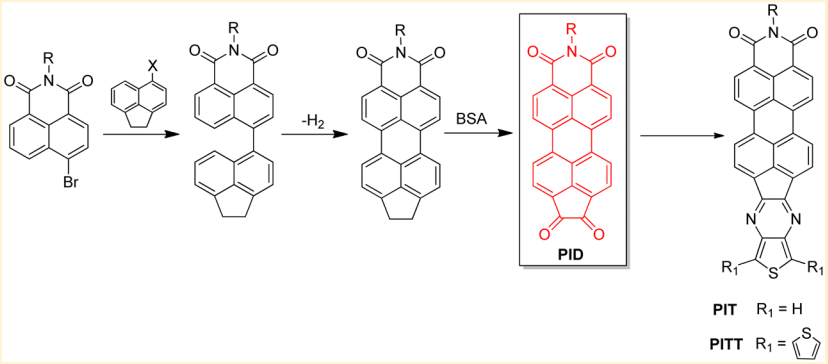

ABSTRACT: There is a great interest in peryleneimide (PI)-containing compounds given their unique combination of good electron accepting ability, high abosorption in the visible region, and outstanding chemical, thermal, and photochemical stabilities. Thus, herein we report the synthesis of perylene imide derivatives endowed with a 1,2-diketone functionality (**PIDs**) as efficient intermediates to easily access peryleneimide (PI)-containing organic semiconductors with enhanced absorption cross-section for the design of tunable semiconductor organic materials. Three processable organic molecular semiconductors containing thiophene and terthiophene moieties, **PITa**, **PITb**, and **PITT**, have been prepared from the novel **PIDs**. The tendency of these semiconductors for molecular aggregation have been investigated by NMR spectroscopy and supported by quantum chemical calculations. 2D NMR experiments and theoretical calculations point to an antiparallel π-stacking interaction as the most stable conformation in the aggregates. Investigation of the optical and electrochemical properties of the materials is also reported and analyzed in combination with DFT calculations. Although the derivatives presented here show modest electron mobilities of $\sim 10^{-4}$ $cm^2V^{-1}s^{-1}$, these preliminary studies of their performance in organic field effect transistors (OFETs) indicate the potential of these new building blocks as n-type semiconductors.

INTRODUCTION

Organic electronics, which exploits organic molecular materials as semiconductors and active elements in devices, is an important growing field of research.[1−8] During the last decades, great effort has been devoted to the design of both hole-conducting (p-type) and electron-conducting (n-type) organic semiconductors, which are required for device applications. Although this research field has evolved dramatically, the search of tunable organic molecules as n-type organic semiconductors is still challenging, due to the scarce molecular diversity of these materials, their limited device performance compared to their p-type homologues, their ambient instability, and the lack of complete understanding of electron transport.[9−15] Perylenediimides and naphthalenediimides (**PDIs** and **NDIs**) are two of the most important families of n-type semiconductors with multiple applications in organic field effect transistors (OFETs),[14,16−20] organic light emitting diodes (OLEDs),[21−23] or organic photovoltaic cells.[24−32] These rylene diimide systems have been proved to be robust, thermally stable, and extremely versatile since their electronic properties can be modulated by well-established organic chemistry, either through modifications on the rylene skeleton or through functionalization on the imide nitrogen atom. In addition, they usually have high electron affinities, which are translated in most cases to remarkable electron transport properties.[33] For example, **NDI** derivatives with fluorinated alkyl chains have demonstrated to perform efficiently in air as n-type semiconductors with mobilities of

Received: September 9, 2016
Published: October 19, 2016

DOI: 10.1021/acs.joc.6b02214
J. Org. Chem. 2016, 81, 11256−11267

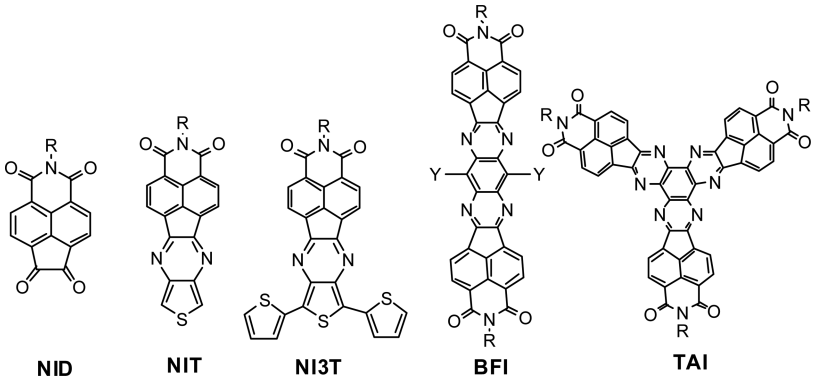

Figure 1. Structure of naphthalene imide dione (**NID**) and some derivatives obtained from this diketone.

Scheme 1. General Route to New Perylene Imide Derivatives (PIT and PITT)

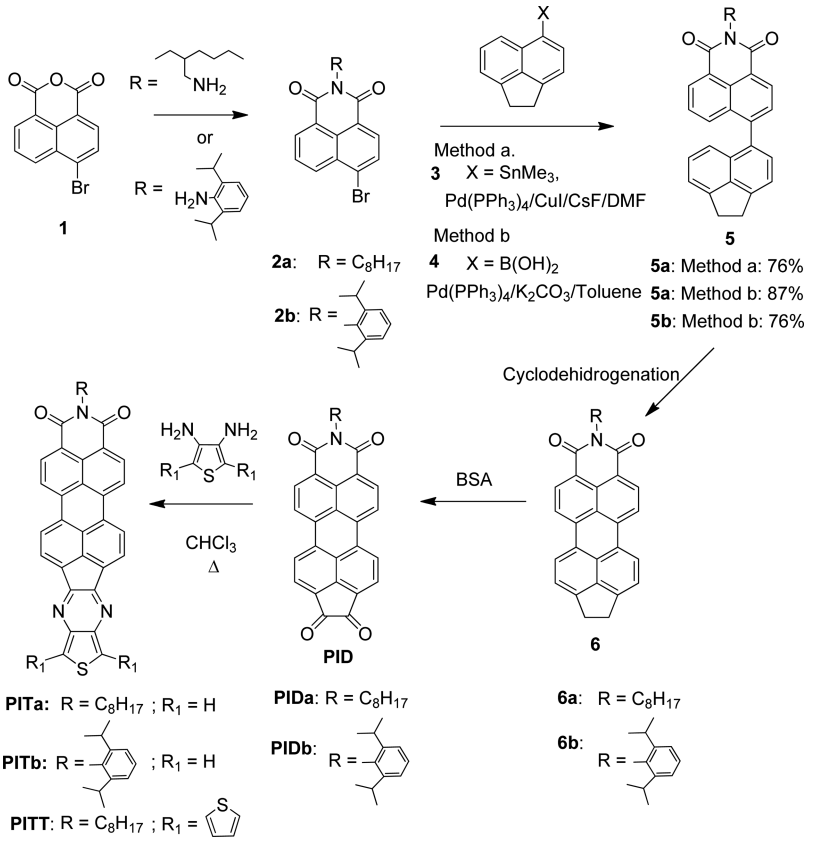

0.12−0.57 $cm^2V^{-1}s^{-1}$, while functionalization on the **NDI** core with electron withdrawing groups, such as chloro[34,35] or cyano,[36,37] renders also air-stable n-type semiconductors with mobilities even surpassing 1 $cm^2V^{-1}s^{-1}$ in thin film devices and up to 8.6 $cm^2V^{-1}s^{-1}$ for single crystals NDI-FETs.[38,39] Similar electronic performances have been reported for **PDI** derivatives,[40] with air-unstable field-effect mobilities surpassing 2 $cm^2V^{-1}s^{-1}$ for alkyl-substituted **PDIs**[41] and air-stable mobilities higher than 1 $cm^2V^{-1}s^{-1}$ in the case of fluoro-alkyl substituted derivatives.[42,43] However, functionalization on the bay area of **PDIs** has been less efficient than that in **NDIs** due to the distortion of the π-conjugated core, remaining only flat in those systems substituted with cyano[44,45] and fluoro[42,43] groups. For this reason, the search for different strategies to modulate the frontier molecular orbitals of **PDIs** is of prime interest. In this sense, in the past few years we have synthesized oligothiophene-naphthalimide and peryleneimide assemblies with good performances in OFETs,[46,47] in which both donor and acceptor moieties are directly conjugated through imidazole rigid linkers. It was found that the absence of skeletal distortions allows closer intermolecular $\pi-\pi$ stacking and enhances intramolecular π-conjugation, while distortion from planarity leads to interruption of the π-electron orbital overlap and can adversely affect charge transport.[42,43,48] In order to get planar analogues, we described the synthesis of a naphthalimide derivative endowed with a 1,2-diketone functionality (**NID**), as a precursor of a family of oligothiophene-naphthalimide assemblies connected through pyrazine linkers (**NIT** and **NI3T**, Figure 1) with completely planar molecular skeletons, which promote good film crystallinity and low reorganization energies for both electron and hole transport.[49,50]

DOI: 10.1021/acs.joc.6b02214
J. Org. Chem. 2016, 81, 11256−11267

Simultaneously, Jenecke and colleagues[51] reported a synthetically tunable tetraazaanthracene core (**BFI**) with two naphthalene imide units based in dione **NID**, creating large rigid ladder-type structures as promising *n*-type materials for organic electronics and nonfullerene photovoltaics. New high-mobility n-type conjugated polymers were also developed based on this versatile synthon.[52]

Thus, in the search for larger planar building blocks with red-shifted absorption for the design of tunable semiconductor organic materials, we describe in this communication the synthesis of **PID** (Scheme 1), the first reported extension of a perylene diimide analogous to previously synthesized naphthalene dione **NID**. The interest in perylenimide (**PI**)-containing compounds is due to the unique combination of good electron accepting ability, high absorption in the visible region, and outstanding chemical, thermal, and photochemical stabilities. Their extended aromaticity together with the possibilities for functionalization make them good candidates for potential applications in electronic materials, sensors, and photovoltaics.[31,53] They also constitute accessible building blocks for the synthesis of extended heteroacenes and heteroarenes, systems highly used in the past decade in thin film transistors with good performance.[54] Herein, we report in detail the design, synthesis, and structural characterization of two perylene imide diones (**PID**) with different substituents at the imide nitrogen and prove the potential of these building blocks, among others, for the synthesis of new assemblies based on peryleneimides fused with electroactive moieties through pyrazine spacers. Thus, new peryleneimides linked to thiophene and terthiophene moieties through pyrazine spacers (**PIT** and **PITT**) have been synthesized, and the preliminary investigation of their optical and electrochemical properties is presented.

RESULTS AND DISCUSSION

As stated before, the synthesis of **PIT** and **PITT** was carried out starting from **PIDs** (Scheme 1). Dione **PIDa** was synthesized by using the synthetic strategy depicted in Scheme 1. First, imide **2a** was obtained by reaction of anhydride **1** with 2-ethylhexylamine, in 98% yield. Alkyl chains in the imide moiety were introduced for solubility purposes.

The synthesis of monoimide **5** was carried out by two alternative procedures, based on palladium catalyzed cross-coupling reactions between brominated naphthalimides (**2a**,**b**) and either stannyl derivative **3** or boronic acid derivative **4**. The previously unknown acenaphthene 5-trimethyltin **3** was synthesized by reaction of 5-bromoacenaphthene[55] with ^{t}BuLi and Me_3SnCl with high yield (95%). On the other hand, boronic acid **4** was obtained also from 5-bromoacenaphthene by treatment of the organollithium derivative with triisopropoxiborane and HCl (10%), in higher yield in comparison with the procedure previously described (70% vs 45%).

$Pd(PPh_3)_4$ catalyzed Stille reaction between monostannane **3** and imide **2a** in toluene afforded product **5a** in a very low yield. However, when the reaction was carried out in the presence of CuI and CsF[56,57] (5% $Pd(PPh_3)_4$, 20% CuI, and 2 mol of anhydrous CsF) in DMF at 55 °C, **5a** could be obtained in good yield (76%). On the other hand, Suzuki reaction of boronic acid **3** in toluene with the same catalyst led to precursor **5a** with an even better yield (87%). Therefore, both methods are feasible for the synthesis of derivative **5a**.

Imide **5a** was obtained as a bright yellow solid and was completely characterized by the usual spectroscopic techniques. Its ^{1}H NMR spectrum shows the characteristic singlet corresponding to the methylene protons of the acenaphthene unit and a multiplet assignable to the N−CH_2− of the alkyl chain at 4.34−4.02 ppm. The rest of the aromatic and aliphatic protons are in the usual range. In the ^{13}C NMR, the presence of the two imide groups at 164.7 and 164.6 ppm can be observed.

For the synthesis of perylene derivative **6a**, we tested the usual reaction conditions based on the use of bases such as KOH, K_2CO_3/ethanolamine, ^{t}BuOK/DBN, or DBU.[58−60] After several attempts using different reaction conditions, product **6a** could be obtained with low yield (20%) by treatment of **5a** with ^{t}BuOK/DBN at 140 °C. Product **6a** was isolated from a complex mixture in which saponification products of the imide could be detected, and therefore, similar reaction conditions were tested using the more robust *N*-arylimide analogue **5b**.[61] Thus, imide **5b** was obtained in a good yield by Suzuki reaction of bromoderivative **2b**[62] with boronic acid **4** (Scheme 1). The subsequent treatment of **5b** with ^{t}BuOK/DBN at 140 °C led only to perylenimide **6b** in 23% yield after silica gel chromatography.

In view of these results, we turned our attention to the Scholl reaction[63−66] to perform the cyclodehydrogenation process. The Scholl oxidation, which generates a new C−C bond between two unfunctionalized aryl carbon atoms, is known to be somewhat erratic.[67] However, it has been profusely used by Müllen and co-workers for the preparation of large polycyclic aromatic hydrocarbons (PAHs) from branched polyphenylenes.[65,68−71] Thus, we first evaluated the common reaction conditions ($FeCl_3$/acetonitrile)[72,73] with imide **5a**, but only oligomeric material could be isolated. Other reagents such as $CuCl_2$, Cu(OTf),[74,75] or DDQ/CH_3SO_3H[76] did not produce detectable quantities of the desired product. In our hands, the best results were obtained by using $AlCl_3$. Reaction in refluxing toluene of either **5a** or **5b** with $AlCl_3$ yielded after 3 h perylenes **6a** and **6b** with 30% and 10% yield respectively, together with starting material (40 and 30% respectively) and oligomeric fractions. The use of chlorobenzene instead of toluene as the solvent allowed for the increase of the yield of *N*-arylimide **6b** (20%), with a 33% recovery of starting material. However, remarkably, imide **6a** was satisfactorily obtained under these reaction conditions with an excellent yield (80%), after column chromatography.

Both perylenes obtained, **6a** and **6b**, present quite good solubility in different solvents such as DCM, chloroform, toluene, AcOEt, or THF and could be characterized by spectroscopic and spectrometric methods. They exhibit similar features in their ^{1}H NMR spectra. ^{13}C NMR was carried out only on perylene **6b**, and HRMS were satisfactory for both perylenes. Perylenes **6a**,**b** were further oxidized with benzeneseleninic anhydride (BSA) in chlorobenzene to afford diones **PIDs** after chromatography in good yield. Both diketones could be characterized by analytical and spectroscopic methods. ^{13}C NMR of compound **PIDb** was carried out in chloroform solution showing the carbonyl and imide groups at 187.2 and 163.6 ppm, respectively.

Diketones **PIDs** represent unique and versatile building blocks for the design of new π-conjugated, electroactive, and multichromophoric systems for optoelectronic applications. In this context, fused-ring thieno[3,4-*b*]pyrazines have been shown to be suitable monomeric units in low band gap conjugated polymers.[77−79] Thus, we choose the condensation reaction between **PIDs** and diaminothiophene derivatives to check the potential of the novel building blocks for the synthesis of new

DOI: 10.1021/acs.joc.6b02214
J. Org. Chem. 2016, 81, 11256−11267

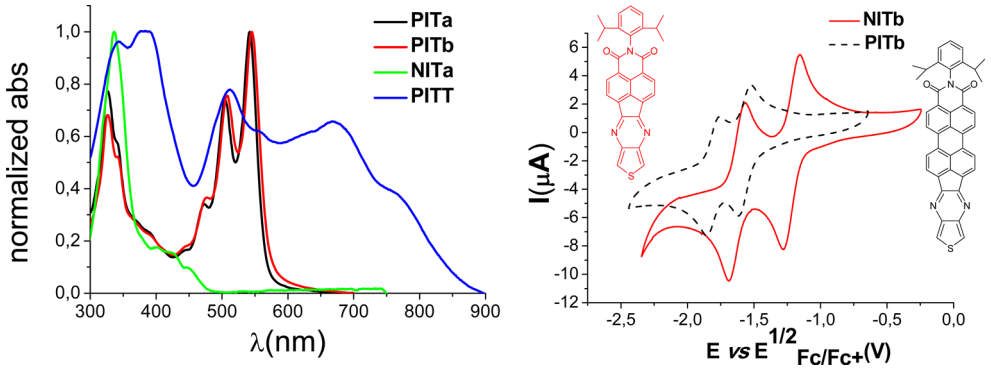

Figure 2. Left: UV−vis absorption spectra of **PIT**, **NIT**, and **PITT** in DCM. Right: comparative voltamperogramms of **PITb** and **NITb**. Cyclic voltammetry in DCM/TBAPF6 (0.1 M) at a scan rate of 100 mV/s using Pt as working and counter electrodes and Fc/Fc^+ as reference.

Table 1. UV−Vis Absorption and Electrochemistry Data[a]

	$E^{1/2}_{redI}$ (V)	$E^{1/2}_{redII}$ (V)	λ_{max} (nm)	$\varepsilon_{\lambda_{max}}$[e] ($cm^{-1}$ M^{-1})	$E_{GAP}{}^{OP}$ (V)	LUMO[b] (eV)	HOMO[c] (eV)
PITb	−1.04	−1.28	545	1.21×10^4	1.94	−3.40 (−3.18)	−5.34 (−5.64)
NITb	−0.95	−1.33	336	5.12×10^5	2.51	−3.49 (−3.01)	−6.00 (−6.22)
PITT	−1.11[d]	−1.41	383	9.1×10^3	1.43	−3.33 (−3.19)	−4.76 (−5.03)

[a]Cyclic voltammetry in DCM/TBAPF6 (0.1 M) at a scan rate of 100 mV/s using Pt as working and counter electrode and SCE as reference (0.52 V vs Fc/Fc^+). [b]LUMO level estimated versus the vacuum level from $E_{LUMO} = -4.44$ eV-eE_{red1}. [c]Estimated from HOMO = LUMO − $E_{GAP}{}^{OP}$. (DFT//B3LYP/6-31G** theoretical data are shown in parentheses.) [d]E_{red} irreversible. [e]Calculated with a linear regression to Lambert−Beer law.

assemblies based on perylene imides fused with thiophene moieties through pyrazine spacers.

Perylene-oligothiophene assemblies **PITa**, **PITb**, and **PITT** were obtained by reaction of diketones **PIDs** with the corresponding diamine derivative in chloroform solution. All compounds were partially soluble in chlorinated solvents such as DCM, chloroform, chlorobenzene, and dichlorobenzene and nonsoluble in polar solvents such as acetonitrile and MeOH. As is characteristic, ^1H NMR spectra of **PIT** compounds exhibit at 7.96 ppm the singlet of the thiophene moiety. For all of them, aromatic protons appear as broad signals in the usual range. ^{13}C NMR could only be obtained of **PITb**. However, additional analytical evidence for these novel systems was provided by high resolution mass spectrometry.

The optical and electronic properties of the novel fused thieno[3,4-*b*]pyrazines **PITs** and **PITT** have been analyzed by UV−visible spectroscopy, cyclic voltammetry, and theoretical calculations. Naphthalimides **NITs** (**NITa**, R = C_8H_{17} and **NITb**, R = $C_{12}H_{15}$, Figure 1) have been also synthesized as previously described by some of us[49,50] and included in this study for comparison purposes (See all figures in SI). The UV−vis spectra of **PITa** and **PITb** in different solvents show identical features regardless of the substituents on the imide N atoms (Figure 2). Both **PIT** derivatives exhibit the characteristic absorption of perylene imide moieties with maxima at 507 and 545 nm that can be ascribed to the 0−0 and 0−1 vibronic bands of the S0−S1 transition, respectively, while the observed absorption band with maxima at 476 nm is attributed to the electronic S0−S2 transition. These absorptions are significantly red-shifted in comparison with that of naphthalimide analogues (**NIT**) with a maximum of the lowest-energy absorptium band at 450 nm. The UV−vis spectrum of **PITT** is especially remarkable. It presents maxima at 342 and 383 nm together with the above-mentioned perylene imide bands at 511 and 555 nm, but in addition, it exhibits a broad absorption centered at approximately 668 nm that extends up to 900 nm and which can be assigned to an intramolecular charge-transfer (ICT) excitation (Figure 2).

The redox behavior of the novel systems was investigated by cyclic voltammetry (CV) measurements (Figure 2 and Figures 7−11 in Supporting Information). Both **PIT** exhibit two reversible reduction processes, due to the perylene imide moiety, within the solvent/electrolyte window range. In contrast, **PITT** displays quasi-irreversible reduction waves. From these data, together with the onset of the absorption spectra, the LUMO and HOMO energies were estimated using standard approximations and compared with that obtained from theoretical calculations (see Table 1 and SI for details). Thus, by comparing the **PITb** derivative with the naphthalene imide analogue **NITb** (Table 1), as a representative, it is observed that the LUMO energies are only slightly affected by the increasing of the core size. Therefore, the HOMO−LUMO gap decrease is associated with the destabilization of the HOMO in **PIT** derivatives with a larger π-conjugated skeleton. On the other hand, oligothiophene-perylene **PITT** presents a similar LUMO energy level, but the HOMO level is more destabilized as the oligothiophene fragment is extended.

These results can be rationalized in terms of the different topologies of the frontier orbitals. Note that the LUMOs are more localized at the ryleneimide moieties, whereas the HOMOs are localized over the entire molecular π-frameworks (Figure 3). In the case of **PITT**, HOMO is localized primarily on the oligothiophene chain as for the previously described **NI3T** derivative.[9]

It is worth pointing out that the LUMO values determined for **PIT** and **PITT** derivatives are comparable to those of state-of-the-art n-type semiconductors.[79] In fact, we already reported that **NIT** derivatives with analogous LUMO values behaved as n-type semiconductors in OFETs.[49,50] Interestingly, as the HOMO levels of **PIT** derivatives are destabilized in comparison with that of the parent **NIT** analogues (1.94 V vs 2.51 eV), they approach the Fermi level of Au (5.0 eV), which is beneficial for hole injection and can pave the way for the development of a

DOI: 10.1021/acs.joc.6b02214
J. Org. Chem. 2016, 81, 11256−11267

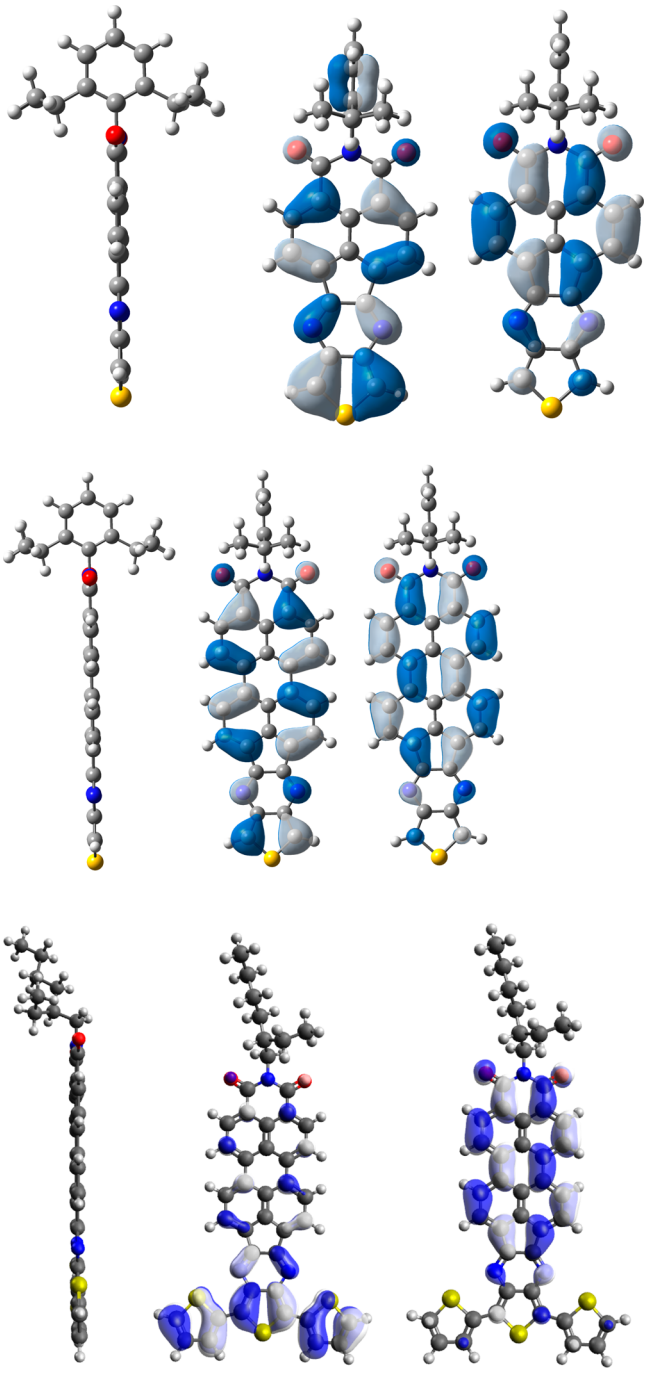

Figure 3. B3LYP/6-31G** optimized structures for **NITb** (top left), **PITb** (middle left), and **PITT** (bottom left), and respective HOMO (center) and LUMO (right) computed orbital topologies.

new family of ambipolar semiconductors when combined with suitable moieties.

In this respect, the internal reorganization energies, λ, for both electron and hole transport in **PIT** and **PITT** derivatives have been computed as previously described[80] and compared with that of **NIT** and **NI3T** analogues. A λ_e of 0.25 and 0.20 eV was determined for **PIT** derivatives which are slightly smaller than the value of 0.34 eV calculated for **NIT**. More similar values are obtained for **PITT** and **NI3T** (λ_e of 0.24 vs 0.25). This behavior is in agreement with that previously observed by us in other thiophene-naphthalimide and thiophene-peryleneimide assemblies.[46] Furthermore, a λ_h as low as 0.10 eV was determined for **PITa**, while a value of 0.16 eV was previously reported for the **NITa** analogue.[49,50] Thus, the extension of the π-conjugated system while keeping a fully planar structure provides low reorganization energies for these new perylene imide derivatives.

We have also explored the molecular aggregation behavior of the novel perylene derivatives. Molecular aggregation in solution, preferentially by π-stacking, is a highly desired property for potential use of these compounds in organic electronics, and we now address this issue.[81] Aggregation can be experimentally studied, among others, by scanning the dependence of the absorption and NMR spectra as a function of concentration. In the concentration range available for UV−vis measurements, no significant change was observed for these derivatives. However, at the higher concentrations (0.3−6 mM) used for NMR experiments carried out at 25 °C, aggregation dependent NMR spectra were observed, this behavior being specially significant for perylene derivatives **6a** and **PITa**. Thus, increasing sample concentrations led to a significant shield of the aromatic protons as well as the methylenes of the acenaphthene unit (Figure 4).

Further insight into the self-aggregation behavior of **PITa** and most probable sites of interactions was provided by 2D NMR Overhauser effect enhancement (NOESY) (Figure 5). NOESY cross-peaks clearly indicate proximity of the aromatic protons of the perylene and the thiophene moieties to the CH_2 and CH of the *N*-alkyl branched chain. Cross-peaks of perylene *d* protons with the alkyl chain protons (*e* and *f*) can be due to intramolecular interaction because the distance between them is shorter than 5 Å as predicted by the computational model, but the other cross-peaks between *e*, *f*, and *a*, *b*, and *c* protons must be explained by self-aggregation.

This spectroscopic finding is in line with the theoretical data obtained on dimer assemblies. Thus, we have theoretically explored the molecular aggregation of the novel perylene derivatives by using ab initio (in all cases a B3LYP functional and 6-31G** basis were used) calculations on dimer models where the alkyl chains were substituted by hydrogen atoms. Two π-stacking conformations (parallel and antiparallel) and three displacement directions (*x*, *y*, and *z* axes) were considered (Figure 6).

Calculations predict that the antiparallel dimer is the most stable conformer, showing no minima in the case of the parallel conformer (even when *y*-axis displacement is considered). The energy profiles depicted in Figure 6 predict that the pure antiparallel π-stacking interaction is the most stable conformation in **NIT** and **PITT** molecules (−5.2 and −6.3 kJ/mol respectively), while the most stable conformation for imide **6** and **PIT** (−11.5 and −3.2 kJ/mol respectively) is found when one of the units of the dimer is slightly *y*-axis displaced (Table 2).

In order to unambiguously determine the self-aggregation of **PITa**, additional calculations were performed, taking into account the interactions observed in its 2D NOESY. In such two-dimensional NMR spectra through-space interactions at proximities of 5 Å or less are observed and are particularly useful for determining the structure of aggregates in solution; so, the starting point in these calculations was a *z*-axis distance of 4 Å for the **PIT-H** model. Parallel and antiparallel conformations energies of **PIT-H** dimers were also calculated when a certain *x*-axis displacement is present (Figure 7). Results show that the parallel displaced **PIT-H** dimer (*x*-axis displacement between 6 and 8 Å) is barely stabilized, less than 1 kJ/mol. However, for the antiparallel dimer two stability zones were found; the first one corresponds to the pure antiparallel dimer (*x*-axis

DOI: 10.1021/acs.joc.6b02214
J. Org. Chem. 2016, 81, 11256−11267

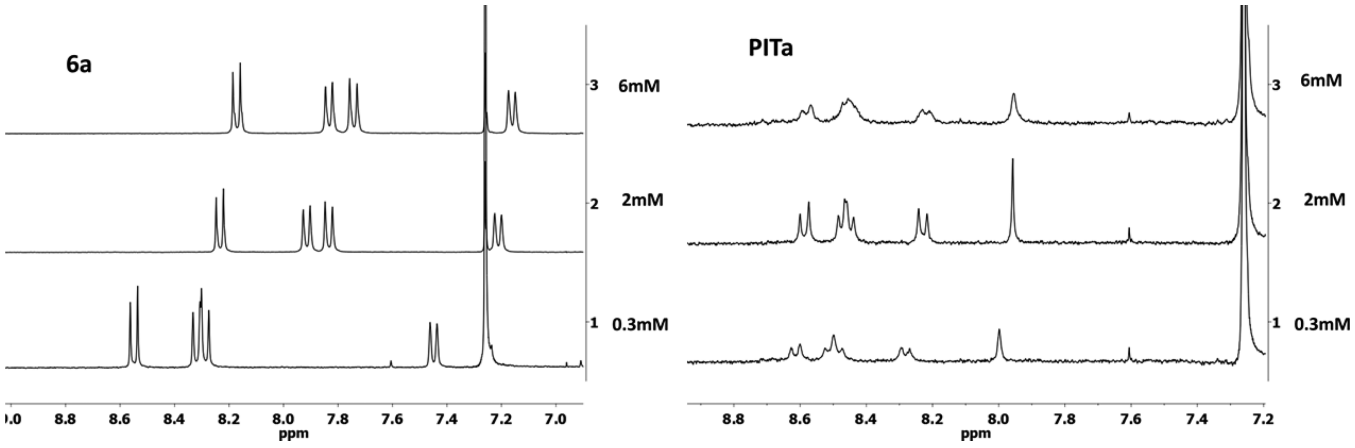

Figure 4. ^{1}H NMR spectra (300 MHz, $CDCl_3$) of the aromatic region of **6a** (left) and **PITa** (right) in $CDCl_3$ solutions at different concentrations.

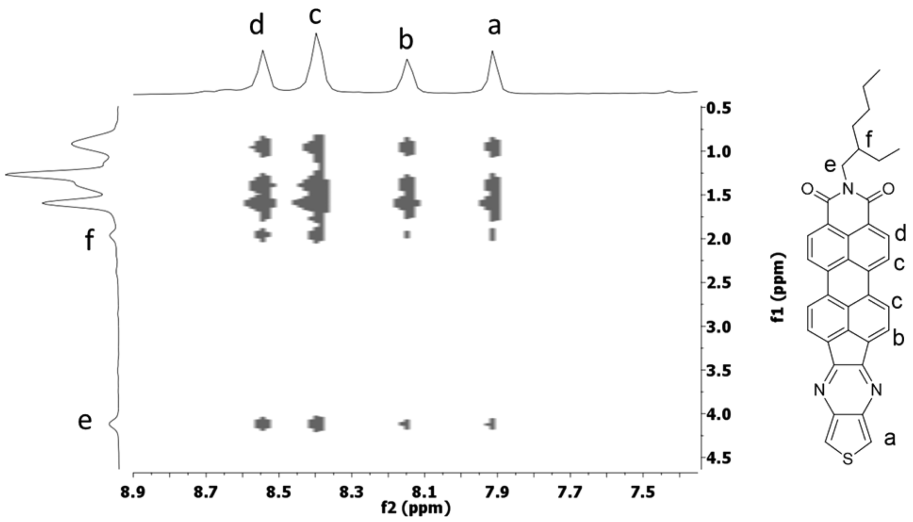

Figure 5. Expansion of NOESY spectrum (700 MHz, $CDCl_3$, 6 mM) of **PITa**.

displacement is equal to 0), and the second one is observed when the *x*-axis is displaced in the 7.5 to 10 Å range (Figure 7). Assuming these theoretical models, the only aggregated structure that could explain the NOE effect observed corresponds to an antiparallel mode of aggregation, where the distances between the imide hydrogen and the hydrogens *b* and *c* of the perylene vicinal unit are in the NOE range.

OFET Fabrication and Characterization. Bottom-gate top-contact OTFTs were fabricated using the studied molecules as the active layer. Gate dielectrics (p-doped Si wafers with 300 nm thermally grown SiO_2 dielectric layers) were functionalized either with hexamethyldisilazane (HMDS) or octadecyltrichlorosilane (OTS) self-assembled monolayers. The capacitance of the 300 nm SiO_2 gate insulator was 10 $nFcm^{-2}$. Prior to the surface functionalization, the wafers were solvent cleaned by immersing them twice for 30 s each in EtOH with sonication, drying with a stream of N_2, and treating with UV-ozone for 10 min. The cleaned silicon wafers were treated with hexamethyldisilazane (HMDS) by exposing them to HMDS vapor at room temperature in a closed air-free container under argon and were treated with octadecyltrichlorosilane (OTS) by inmersion in a 3.0 mM humidity-exposed OTS-hexane solution for 1 h, as previously described.[82] Following OTS deposition, the substrates were sonicated with hexane, acetone, and ethanol, and dried with a N_2 stream.

Next, the semiconductors were either drop-casted or vapor-deposited on preheated substrates. After semiconductor deposition, the solution-processed films were annealed under vacuum at selected temperatures and initially analyzed by AFM techniques (Figure 8). OFET devices were completed by gold electrode vapor deposition through a shadow mask to define devices with various channel lengths and channel widths. Devices were characterized under vacuum and ambient conditions in an EB-4 Everbeing probe station with a 4200-SCS/C Keithley semiconductor characterization system. Data obtained are collected in Table 3.

Figure 8 shows AFM images for **PITa** and **PITb** thin films deposited onto HMDS or OTS treated substrates preheated at selected temperatures. In the case of **PITa**, we observe that grain sizes are strongly dependent on the deposition temperature. While small rounded grains are recorded for films annealed at 110 °C, grain sizes of around 0.5 μm are found at higher annealing temperatures. Note, however, that the grain connectivity is poor for 150 °C annealed films. Although the morphology is still far away from optimum, the substitution of the alkyl chain of **PITa** by a phenyl unit, **PITb**, results in well-defined rounded grains presenting better connectivity. The most noticeable morphology change is recorded for the solution processed film of **PITT**, where rod-like grains surpassing 1 μm are observed. These morphology changes parallel those

DOI: 10.1021/acs.joc.6b02214
J. Org. Chem. 2016, 81, 11256−11267

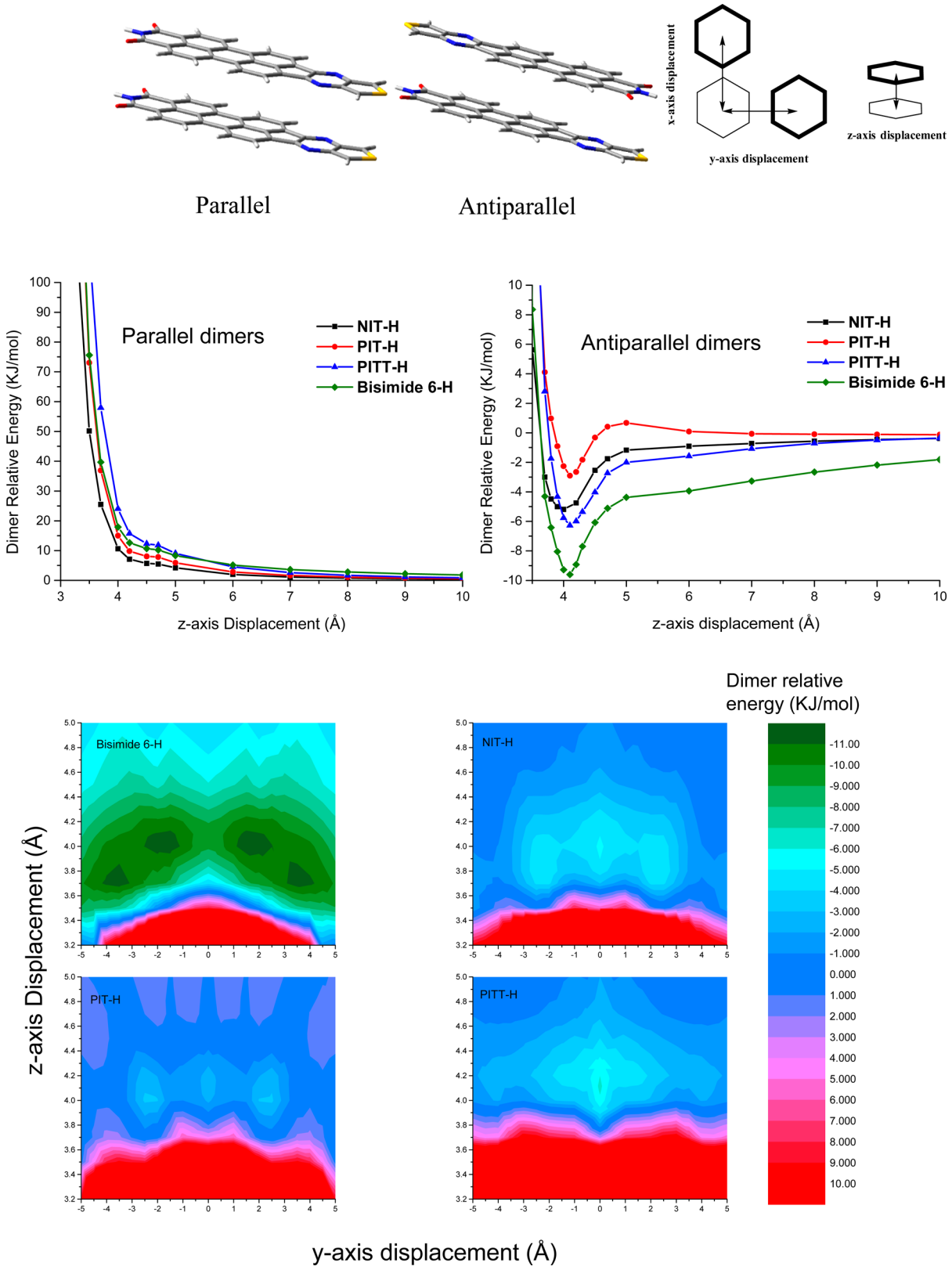

Figure 6. Top: different conformations of dimers of the model **PIT** with hydrogen atoms instead of alkyl chains. Middle: Pure parallel and antiparallel conformation dimer relative energies (*z*-axis only displacement). Bottom: 2D energy surfaces of antiparallel dimer conformations (*z* and *y* axis displacement) (B3LYP/6-31G**).

previously recorded for their homologous **NIT** and **NI3T** derivatives, where rod-like grains are also found for the terthiophene derivative deposited at high temperatures.[49]

Comparing the electrical performances of vapor-deposited films of the studied semiconductors in a OFET geometry (Figure 9), we observe a clear enhancement of the electron field

DOI: 10.1021/acs.joc.6b02214
J. Org. Chem. 2016, 81, 11256−11267

Table 2. Calculated Intermolecular Distances and Energies for the Dimers of the Model Compounds

model compounds	vertical displacement (Å)	horizontal displacement (Å)	energy (kJ/mol)
bisimide 6-H	4	±1.5	−11.5
NIT-H	4.0	0	−5.2
PIT-H	4	±2.5	−3.2
PITT-H	4.1	0	−6.3

effect mobility (×2) of **PITb** (1.2×10^{-4} $cm^2V^{-1}s^{-1}$) with respect to **PITa** (5.8×10^{-5} $cm^2V^{-1}s^{-1}$) when deposited on substrates preheated at 110 °C. This can be ascribed to the formation of rounded well-connected grains in the former, as evidenced by AFM images. Higher substrate temperature during deposition increases **PITa** mobility to values similar to those recorded for **PITb**. This electrical performance is comparable with those previously published for **NIT** semiconductors.[49]

In the case of the terthiophene derivative, films were deposited by drop casting; devices with electron mobilities of 1.2×10^{-4} $cm^2V^{-1}s^{-1}$ were registered. However, despite the presence of the terthiophene moiety, no ambipolar behavior is observed for **PITT** which contrasts with that observed for other donor−acceptor assemblies containing terthiophene moieties.[47] This fact can be rationalized in terms of the antiparallel $\pi-\pi$ stacking conformation of the novel molecules anticipated by theoretical calculations and empirically observed, which does not allow the formation of D and A domains for transporting holes and electrons, respectively.[83]

CONCLUSIONS

In conclusion, the methodology described in this article constitutes an efficient strategy for the synthesis of perylene imide diones, **PID**, as reactive intermediates for the development of new pyrazine fused π-conjugated systems with good electron accepting ability and high absorption in the visible region. Especially noteworthy is the UV−vis absorption of the assembly based on perylenimide and terthiophene which shows an enhanced absorption cross-section from 300 to 900 nm. Aggregation dependent NMR spectra were obtained, thus confirming the characteristic tendency for molecular aggregation through $\pi-\pi$ stacking of this type of flat conjugated perylene-based assemblies. Theoretical calculations predict that the antiparallel π-stacking interaction is the most stable conformation in four tested model naphthalene/perylene-based dimers. The potential of these novel semiconductors has been investigated by using them as active layers in bottom-gate top-contact OTFTs. All of them show n-type mobilities with the highest value of 1.5×10^{-4} cm^2 V^{-1} s^{-1} for the peryleneimide-thiophene assembly **PITa**. This novel building block provides a

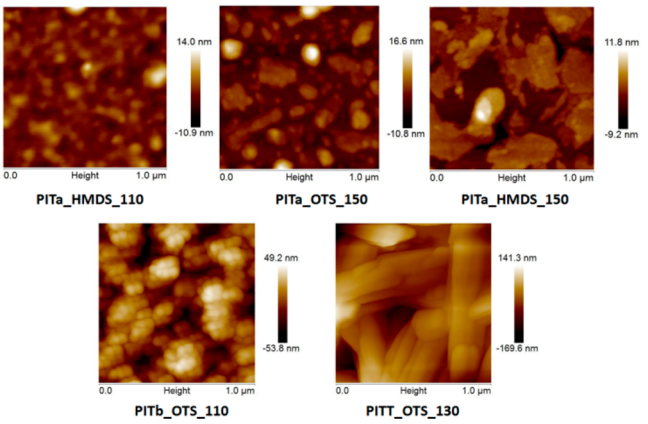

Figure 8. AFM images (5 × 5 μm) of thin films of the studied semiconductors deposited on substrates preheated at the indicated temperatures.

Table 3. OFET Electrical Data for Vapor-Deposited Films (unless Otherwise Specified) of the Indicated Semiconductors Measured in Vacuum

	subst.[a]/T (°C)	μ_e ($cm^2V^{-1}s^{-1}$)	V_T (V)
PITa	H/110	5.8×10^{-5}	31
PITa	O/150	1.5×10^{-4}	36
PITa	H/150	1.1×10^{-4}	33
PITb	O/110	1.2×10^{-4}	25
PITT[b]	O/SP-130	1.2×10^{-4}	8

[a]H, hexamethyldisilazane-treated substrates; O, *n*-octadecyltri-chlor-osilane-treated substrates. [b]SP: solution-processed film.

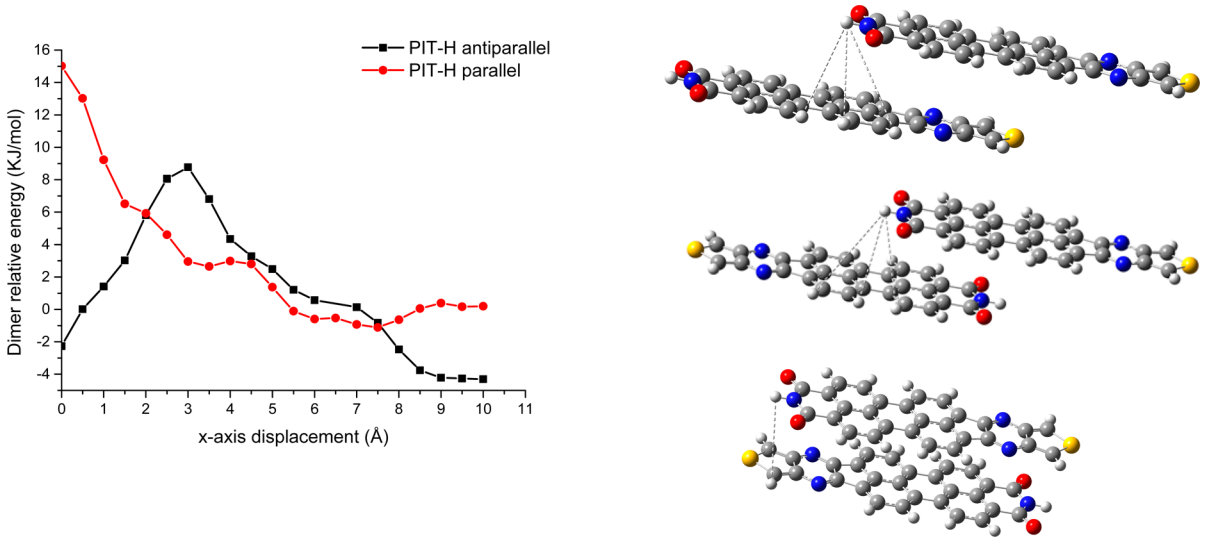

Figure 7. Left: relative energy of parallel and antiparallel **PIT-H** dimers when a *x*-axis displacement is performed. Right: dotted lines represent distances between 4.5 and 5.5 Å. (Top) Parallel stable conformation; (middle and bottom) most stable antiparallel conformations.

DOI: 10.1021/acs.joc.6b02214
J. Org. Chem. 2016, 81, 11256−11267

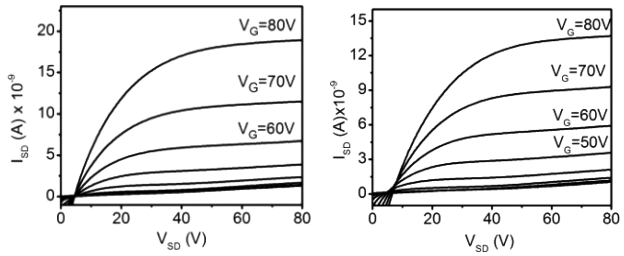

Figure 9. Output plots for vapor-deposited **PITa** FETs grown at 150 °C on HMDS-treated substrates (left) and vapor-deposited **PITb** FETs grown at 110 °C on OTS-treated substrates (right).

playground to prepare a plethora of new materials with different architectures and side chains for electronic applications where n-type materials with enhanced absorption cross-section are needed.

EXPERIMENTAL SECTION

General Methods and Materials. All reactions with air sensitive materials were carried out under Ar using standard Schlenk techniques. TLC was performed using precoated silica gel 60 F254 and developed in the solvent system indicated. Compounds were visualized by use of UV light (λ = 254). 230−400 Mesh silica gel was used for column chromatography.

Toluene and THF were freshly distilled over sodium/benzophenone under nitrogen before use. NBS, $Pd(PPh_3)_4$, trimethyltin chloride, acenaphthene, triisopropoxyborane, 4-bromo-1,8-naphthalicanhydride **1**, 2-ethyl-1-hexylamine, *tert*-butyllithium, K_2CO_3, CuI, 3-bromothiophene, and CsF were purchased from commercial suppliers and used without further purification.

Dione **NIDa**,[50] 5-bromoacenaphthene,[55] thiophene-3,4-diamine,[84] naphthalimide **2a**,[85] imide **2b**,[62] and [2, 2′:5′,2″-terthiophene]-3′,4′-diamine[86] were prepared according to literature methods.

^{1}H NMR and ^{13}C NMR spectra were recorded on a 300 and 500 MHz spectrometer. Chemical shifts are reported in ppm and referenced to the residual nondeuterated solvent frequencies ($CDCl_3$: δ 7.26 ppm for ^{1}H, δ 77.0 ppm for ^{13}C). Mass spectra were recorded by means of MALDI-TOF or FAB/IE techniques. Melting points were collected either in a microscope coupled with a heating plate or using a capillary melting point apparatus and are uncorrected. UV/vis absorption spectra were recorded in 1 cm cuvettes. Infrared spectra are reported in wavenumbers (cm^{-1}). Solids were analyzed on a diamond plate (ATR) or as films on sodium chloride. Cyclic voltammetry experiments were performed with a computer controlled potentiostat in a three electrode single-compartment cell (5 mL). The platinum working electrode consisted of a platinum wire with a surface of A = 0.785 mm^2, which was polished down to 0.5 μm with polishing paste prior to use in order to obtain reproducible surfaces. The counter electrode consisted of a platinum wire, and the reference electrode was a Ag/AgCl secondary electrode. An electrolyte solution of 0.1 M $TBAPF_6$ in freshly distilled and degassed acetonitrile (HPLC) was used in all experiments.

All calculations were performed using the program Gaussian 09, Rev. B.01.[87] In all cases, the functional B3LYP and a 6-31G** (6-31++G** for anions) basis were used following an unrestricted DFT method for the cation and anion radicals. For geometry optimizations, an additional frequency calculation was performed showing no imaginary frequencies confirming the potential energy minimum nature of the geometry. Default options for energy minima search and integral accuracy were applied.

*4-Bromo-N-(2-ethylhexyl)-1,8-naphthalimide (**2a**).*[85] A suspension of 4-bromo-1,8-naphthalicanhydride **1** (2 g, 7.2 mmol) in 60 mL of EtOH was refluxed. Then, 2-ethyl-1-hexylamine (2 mL, 12.1 mmol) was added, and the mixture was heated for 24 h. The solvent was evaporated, and the product was purified by flash column chromatography (SiO_2, hexane/dichloromethane 9:1) to give 2.75 g (98%) as a yellow solid. M.p.: 90−91 °C. ^{1}H NMR (300 MHz, $CDCl_3$) δ (ppm) = 8.62 (d, J = 7.3 Hz, 1H), 8.52 (d, J = 8.5 Hz, 1H), 8.37 (dd, J = 7.9, 2.4 Hz, 1H), 8.00 (dd, J = 7.9, 2.4 Hz, 1H), 7.8−7.74 (m, 1H), 4.19−4.00 (m, 2H), 1.92 (dt, J = 13.0, 6.6 Hz, 1H), 1.48−1.09 (m, 9H), 0.89 (dt, J = 15.5, 7.3 Hz, 6H). ^{13}C NMR (75 MHz, $CDCl_3$) δ (ppm) = 164.3, 133.5, 132.4, 131.6, 131.5, 130.9, 130.5, 129.4, 128.5, 123.5, 122.6, 44.6, 38.3, 31.1, 29.1, 24.4, 23.5, 14.5, 11.0. FTIR (ATR, $CHCl_3$) ν (cm^{-1}) = 2957, 2922, 2859, 1701, 1653, 1581, 1348, 1185 $cm.^{-1}$

*4-Bromo-N-(2,6-diisopropylphenyl)-1,8-naphthalimide (**2b**).*[62] A suspension of 4-bromo-1,8-naphthalicanhydride **1** (1g, 3.6 mmol) in 10 mL of acetic acid and 1.5 mL (7.2 mmol) of 1,6-diisopropylaniline was heated to reflux for 4 days. Then water was added, and the solid was filtered, washed with water, solved in dichloromethane, and dried over $MgSO_4$. The solvent was removed under pressure, and the crude was purified by chromatography (SiO_2, Hexane/dichloromethane, 7:3) to yield 1.07 g (85%) of **2b** as a clear solid. ^{1}H NMR (300 MHz, $CDCl_3$) δ (ppm) = 8.74 (dd, J = 7.3, 1.2 Hz, 1H), 8.67 (dd, J = 8.5, 1.2 Hz, 1H), 8.50 (d, J = 7.9 Hz, 1H), 8.10 (d, J = 7.9 Hz, 1H), 7.91 (dd, J = 8.6, 7.2 Hz, 1H), 7.49 (dd, J = 8.3, 7.2 Hz, 1H), 7.35 (d, J = 7.7 Hz,2H), 2.73 (hept, J = 6.8 Hz, 2H), 1.17 (d, J = 6.8 Hz, 12 H).

*Acenaphthene-5-trimethylstannane (**3**).* A solution of 5-bromoacenaphthene (0.3 g, 1.83 mmol) in 4 mL of anhydrous THF was cooled to −78 °C. Then, 2.6 mL (4.4 mmol) of ^{t}BuLi 1.7 M was very slowly added, under argon. After 2 h, trimethyltin chloride (0.47 g, 2.38 mmol) was added under argon, and the resulting mixture was stirred for 24 h at room temperature. The solvent was evaporated, the mixture dissolved in DCM, washed with water, and dried over anhydrous $MgSO_4$, to give 0.55 g (95%) of **3** as a light brown solid. M.p.: 68−70 °C. ^{1}H NMR (300 MHz, $CDCl_3$) δ (ppm) = 7.53 (m, 1H), 7.51 (s, 1H), 7.40 (t, J = 7.4 Hz, 1H), 7.22 (d, J = 7.2 Hz, 2H), 3.30 (s, 4H), 0.39 (s, 9H). ^{13}C NMR (75 MHz, $CDCl_3$) δ (ppm) = 146.9, 146.8, 145.9, 139.0, 137.1, 136.0, 135.7, 127.7 (2C), 124.20, 122.2, 119.2, 119.1, 119.0, 30.2. FTIR (ATR, $CHCl_3$) ν (cm^{-1}) = 3031, 2978, 2916, 2839, 1600, 1359, 838, 816, 764. MS (EI) m/z: (M^+ 318.09, 18%), 303 (100%), 301 (81%), 299 (39%), 273 (31%), found for $C_{15}H_{18}Sn$ (M^+, 318.04). HRMS (EI) m/z: calculated for $C_{15}H_{18}Sn$, 318.0425; found, 318.0453

*4-Acenaphthene-5-yl-N-(2-ethylhexyl)-1,8-naphthalimide (**5a**).* (a) Suzuki coupling: To a degassed solution of imide **2a** (2.8 g, 7.2 mmol) and acenaphthene-5-boronic acid **4** (1.42 g, 7.2 mmol) in 85 mL of toluene was added 28 mL of a degassed solution of K_2CO_3 (2M) and $Pd(PPh_3)_4$ (832 mg, 0.72 mmol) under argon. The mixture was refluxed overnight. Then, the solvent was evaporated, and the mixture was dissolved in DCM, washed with water, and dried over anhydrous $MgSO_4$. The product was purified (SiO_2, hexane/diethyl ether 8:2) to give 2.9 g (87%) of a yellow solid. (b) Stille coupling: To a degassed solution of imide **2a** (0.85 g, 2 mmol) and acenaphthene-5-trimethyl stannane **3** (0.69 g, 2 mmol) in 7 mL of DMF was added $Pd(PPh_3)_4$ (115 mg, 0.1 mmol), CuI (0.038 g, 0.2 mmol), and CsF (0.61 g, 4 mmol) under argon. The mixture was heated at 55 °C overnight. Then, the solvent was evaporated, the mixture dissolved in DCM, washed with water, and dried over anhydrous $MgSO_4$. The product was purified (SiO_2, hexane/diethyl ether 8:2) to give 0.7 g (76%) of a yellow solid. M.p.: 128−129 °C. ^{1}H NMR (300 MHz, $CDCl_3$) δ (ppm) = 8.70 (d, J = 7.5 Hz, 1H), 8.61 (dd, J = 7.2, 0.9 Hz, 1H), 7.94 (dd, J = 8.4, 0.9 Hz, 1H), 7.82−7.74 (m, 1H), 7.54 (dd, J = 8.4, 7.4 Hz, 1H), 7.44 (q, J = 7.1 Hz, 2H), 7.37−7.27 (m, 2H), 7.10 (m, J = 3.2 Hz, 1H), 4.34−4.02 (m, 2H), 3.50 (s, 4H), 2.04 (dd, J = 12.4, 6.2 Hz, 1H), 1.58−1.18 (m, 8H), 0.96 (dt, J = 14.1, 7.2 Hz, 6H). ^{13}C NMR (75 MHz $CDCl_3$) δ (ppm) = 164.7, 164.6, 147.2, 146.4, 145.3, 139.3, 132.98, 131.8, 131.4, 131.2, 130.9, 130.6, 129.8, 129.0, 128.6, 126.7, 123.0, 122.0, 120.7, 119.8, 119.0, 44.2, 38.0, 30.9, 30.6, 30.3, 28.8, 24.2, 23.2, 14.22, 10.8. Anal. Calculated for $C_{32}H_{31}NO_2$: C, 83.26; H, 6.77; N, 3.03. Found: C, 83.56; H, 6.88; N, 3.12. HRMS (EI) m/z: calculated for $C_{32}H_{31}NO_2$, 461.2349; found, 461.2350.

*4-Acenaphthene-5-yl-N-(2,6-diisopropylphenyl)-1,8-naphthalimide (**5b**).* To a degassed solution of imide **2b** (0.828 g, 1.9 mmol) and acenaphthene-5-boronic acid (0.376 g, 1.9 mmol) in 25 mL of toluene was added 9.5 mL of a degassed solution of K_2CO_3 (2M) and $Pd(PPh_3)_4$ (0.219 mg, 0.19 mmol) under argon. The mixture was refluxed overnight. Then, the solvent was evaporated, and the mixture was dissolved in DCM, washed with water, and dried over anhydrous

DOI: 10.1021/acs.joc.6b02214
J. Org. Chem. 2016, 81, 11256−11267

$MgSO_4$. The product was purified (SiO_2, hexane/DCM 8:2) to give 0.9 g (93%) of a yellow solid. M.p.: 318−320 °C. ^{1}H NMR (300 MHz, $CDCl_3$) δ (ppm) = 8.77 (d, J = 7.5 Hz, 1H), 8.68 (dd, J = 7.3, 1.2 Hz, 1H), 8.03 (dd, J = 8.5, 1.2 Hz, 1H), 7.85 (d, J = 7.5 Hz, 1H), 7.62 (dd, J = 8.5, 8.4 Hz, 1H), 7.49 (m, 3H), 7.37 (m, 4H), 7.11 (m, 1H), 3.47 (s, 4H), 2.76 (hept, J = 6.8, 2H), 1.13 (m, 12H). ^{13}C NMR ($CDCl_3$, 75 MHz) δ (ppm) = 164.3, 164.2, 147.3, 146.4, 145.7, 139.3, 133.4, 131.7, 130.9, 130.6, 129.7, 129.5, 129.1 129.0, 128.6, 126.7, 124.0, 122.9, 121.9, 120.7, 119.9, 119.0, 53.4, 30.6, 30.3, 29.2, 24.0. FTIR (ATR, $CHCl_3$) ν (cm^{-1}): 2964, 1708, 1667, 1588, 1356, 1237, 784. MS (EI) m/z: 510 (M+1, 38%), (M^+, 509.2, 97%), 492 (25%), 467 (38%), 468 (100%), 349 (29%) calculated for $C_{36}H_{31}NO_2$ (M^+, 509.6). HRMS (EI) m/z: calculated for $C_{36}H_{31}NO_2$, 509.2349; found, 509.2348

*N-(2-Ethylhexyl)-1,2-dihydrocyclopenta[cd]perylene-7,8-dicarboximide (**6a**).* Method a: A mixture of potassium *tert*-butoxide (0.7 g, 6 mmol) and DBN (0.5 g, 6 mmol) was heated for 1 h to 140 °C under argon. Then, imide **5**(100 mg, 0.21 mmol) was added in one portion, and the mixture was further heated for 3 h at 140 °C. The reaction mixture was cooled to room temperature, and the suspension was dissolved in DCM, washed with water, and dried over anhydrous $MgSO_4$. The crude material was purified (SiO_2, hexane/diethyl ether 8:2) to give 20 mg (20%) of **6a** as a dark red solid. Method b: To a solution of $AlCl_3$ (520.5 mg, 3.9 mmol) in 60 mL of anhydrous chlorobenzene, imide **5** (200 mg, 0.43 mmol) was added slowly in 10 mL of chlorobenzene, and the mixture was heated to reflux for 6 h. Then, the crude was cooled to room temperature, and water was added. The mixture was extracted and dried over $MgSO_4$, and the solvent was evaporated. The red solid was purified by chromatography (SiO_2, dichloromethane) to give 160 mg (80%) of **6a** as a red solid. M.p.: 244−245 °C. ^{1}H NMR (300 MHz, $CDCl_3$) δ (ppm) = 8.54 (d, 2H, J = 8 Hz), 8.3 (dd, 4H, J = 7.5 Hz), 7.45 (d, 2H, J = 8 Hz), 4.14 (t, 2H), 3.48 (s, 4H), 1.97 (m, 1H), 1.33 (m, 8H), 0.91 (m, 6H). FTIR (ATR, CH_2Cl_2): 2922, 2854, 1684, 1644, 1582, 1459, 1380, 1353 cm^{-1}. ^{13}C NMR ($CDCl_3$, 125 MHz) δ (ppm) = 164.3, 149.6, 139.4, 136.9, 130.9, 130.0, 126.9, 125.5, 124.7, 120.9, 119.7, 118.8, 44.2, 38.2, 31.1, 31.0, 29.8, 28.9, 24.3, 23.3, 14.3, 10.8. MS (EI) m/z: (M^+, 459.3, 29%), 347 (71%), 277 (30%), 167 (33%), 149 (43%), 95 (100%), 82 (35%) calculated for $C_{32}H_{29}NO_2$ (M^+, 459.2). HRMS (EI) m/z: calculated for $C_{32}H_{29}NO_2$, 459.2193; found, 459.2192

*N-(2,6-Diisopropylphenyl)-1,2-dihydrocyclopenta[cd]perylene-7,8-dicarboximide (**6b**).* Method a: A mixture of potassium *tert*-butoxide (628 mg, 5.6 mmol) and DBN (462 mg, 3.72 mmol) was heated for 1 h to 140 °C under argon. Then, imide **5b** (100 mg, 0.19 mmol) was added in one portion, and the mixture was further heated for 3 h at 140 °C. The reaction mixture was cooled to room temperature, and the suspension was dissolved in DCM, washed with water, and dried over anhydrous $MgSO_4$. The crude material was purified (SiO_2, dichloromethane) to give 20 mg (20%) of a dark red solid. Method b: To a solution of $AlCl_3$ (460 mg, 3.4 mmol) in 15 mL of anhydrous chlorobenzene, imide **5b** (200 mg, 0.38 mmol) was added slowly in 8 mL of chlorobenzene, and the mixture was heated to reflux for 3 h. Then, the crude was cooled to room temperature, and water was added. The mixture was extracted and dried over $MgSO_4$, and the solvent was evaporated. The red solid was purified by chromatography (SiO_2, dichloromethane) to give 40 mg (20%) of **6b** as a red solid, accompanied by starting material and oligomeric byproducts. M.p: >320 °C. ^{1}H NMR (300 MHz, $CDCl_3$) δ (ppm) = 8.63 (d, J = 8.0 Hz, 2H), 8.34 (d, J = 7.6 Hz, 4H), 7.46 (d, J = 7.4 Hz, 1H), 7.34 (d, J = 7.8, 2H), 3.48 (s, 4H), 2.77 (hept, J = 6.8 Hz,4H),1.18 (d, J = 6.8 Hz,12H). ^{13}C NMR ($CDCl_3$, 125 MHz) δ (ppm) = 164.1, 149.8, 145.7, 139.9, 137.9, 132.0, 131.3, 129.3, 127.9, 126.0, 125.3, 123.9, 121.3, 121,2, 120.3, 119.2, 31.2, 29.1, 24.0. FTIR (ATR, $CHCl_3$) ν (cm^{-1}): 2957, 2925, 2855, 1715, 1647, 1459, 1375, 1241, 1181, 1082 cm^{-1}. MS (EI) m/z: (M^+, 507.2, 53%), 464 (18%), 466 (16%), 348 (30%), 347 (100%) calculated for $C_{36}H_{29}NO_2$ (M^+, 507.2). HRMS (EI) m/z: calculated for $C_{36}H_{29}NO_2$, 507.2193; found, 507.2191.

PIDa. A solution of 160 mg (0.34 mmol) of imide **6a** and 407 mg of BSA (1.12 mmol) in 16 mL of anhydrous chlorobenzene was heated at 130 °C overnight. The solution reached an orange color. Then, the mixture was cooled to room temperature, and the solvent was removed in vacuo. The red solid was dissolved in dichloromethane and washed with water. The organic layer was dried with $MgSO_4$, and the solvent was once again evaporated. The red solid was purified by chromatography (SiO_2, dichloromethane/MeOH, 95:5) to give 192 mg (78%) of **PIDa** as a red solid. M.p: >320 °C. ^{1}H NMR (300 MHz, $CDCl_3$) δ = 8.70 (d, 2H, J = 8 Hz), 8.58 (dd, 4H, J = 7.9 Hz, J = 2.2 Hz), 8.17 (d, 2H, J = 7.7 Hz), 4.15 (m, 2H), 1.02 (m, 1H), 1.34 (m, 8H), 0.92 (m, 6H). FTIR (ATR, CH_2Cl_2): 3061, 2958, 2926, 2856, 1730, 1696, 1655, 1608, 1585, 1438, 1413, 1381, 1356, 1316, 1240, 1200, 1173, 1126, 1096, 1071, 1019, 851, 826, 788, 746, 687 cm^{-1}. HRMS (EI) m/z: calculated for $C_{32}H_{25}NO_4$, 487.1778; found, 487.1770.

PIDb. A solution of 78 mg (0.15 mmol) of imide **6b** and 180 mg of BSA (0.49 mmol) in 8 mL of anhydrous chlorobenzene was heated at 130 °C overnight. The solution reached an orange color. Then, the mixture was cooled to room temperature, and the solvent was removed under vacuum. The red solid was dissolved in dichloromethane and washed with water. The organic layer was dried with $MgSO_4$, and the solvent was once again evaporated. The red solid was purified by chromatography (SiO_2, dichloromethane) to give 79 mg (95%) as a red solid. M.p: >320 °C. ^{1}H NMR (300 MHz, $CDCl_3$) δ = 8.76 (d, 2H, J = 8 Hz), 8.63 (dd, 4H, J = 7.9 Hz, J = 2.1 Hz), 8.2 (d, 2H,J = 7.7 Hz), 7.51 (m, 1H), 7.36 (d, 2H, J = 7.8 Hz), 2.73 (m, 2H), 1.18 (d, 12H, J = 6.8 Hz). ^{13}C NMR ($CDCl_3$, 175 MHz) δ (ppm) = 187.2, 163.6, 145.7, 135.5, 135.1, 133.8, 132.2, 130.8, 129.9, 129.3, 128.7, 126.5, 124.3, 124.2, 123.7, 123.6, 122.9, 96.2, 29.3, 24.1. FTIR (ATR, CH_2Cl_2): 2951, 2926, 2852, 1731, 1704, 1666, 1463, 1176, 1148, 1118, 1103 cm^{-1}. MS (EI) m/z: (M^+, 535.19, 31%), 508 (37%), 391 (37%), 361 (37%), 281 (33%), 219 (58%), 207 (100%) calculated for $C_{26}H_{25}NO_4$ (M^+, 535.17). HRMS (EI) m/z: calculated for $C_{36}H_{25}NO_4$, 535.1784; found, 535.1779.

PITa. Under argon atmosphere, 3,4-diamine thiophene, 15 mL of anhydrous chloroform, 40 mg (0.082 mmol) of **PIDa**, and a catalytic amount of *p*-TSA were heated to 50 °C and left stirring overnight. Then, the crude was washed with $NaHCO_3$ and water. The organic layer was dried over $MgSO_4$, and the solvent was removed under pressure. The mixture was solved in dichloromethane and precipitated and washed with MeOH to yield 24 mg (52%) of a dark solid. M.p: >200 °C. ^{13}C NMR could not be performed due to the precipitation of the sample in all solvents. ^{1}H NMR (300 MHz, $CDCl_3$) δ (ppm) = 8.59 (bs, 2H), 8.48 (bs, 4H), 8.25 (bs, 2H), 7.96 (s, 2H), 4.15 (m, 2H), 1.97 (m, 1H), 1.42 (m, 8H), 0.91 (m, 6H). FTIR (ATR, CH_2Cl_2): 2958, 2924, 2854, 1737, 1694, 1653, 1584, 1516, 1459, 1413, 1380, 1353, 1316, 1260, 1170, 1095, 1060, 1020, 802, 752, 693, 607, 568 cm^{-1}. HRMS (EI) m/z: calculated for $C_{36}H_{27}N_3O_2S$, 565.1818; found, 565.1817.

PITb. Under argon atmosphere, 3,4-diamine thiophene, 7 mL of anhydrous chloroform, 20 mg (0.039 mmol) of the dione **PIDb**, and a catalytic amount of *p*-TSA were heated to 50 °C and left stirring overnight. Then, the crude was washed with $NaHCO_3$ and water. The organic layer was dried over $MgSO_4$, and the solvent was removed under pressure. The mixed was solved in dichloromethane and precipitated and washed with MeOH to yield 91% (21 mg) of a dark red solid. M.p: >200 °C. ^{1}H NMR (300 MHz, $CDCl_3$) δ = 8.70 (bs, 2H), 8.56 (bs, 4H), 8.29 (bs, 2H), 7.97 (s, 2H), 7.50 (m, 1H), 7.37 (d, 2H, J = 7.3 Hz), 2.79 (m, 2H), 2.02 (m, 1H), 1.20 (d, 12H, J = 6.7 Hz). FTIR (ATR, CH_2Cl_2): 2960, 2925, 2866, 1704, 1665, 1584, 1516, 1549, 1412, 1359, 1321, 1246, 1194, 1175, 1141, 1092, 1050, 846, 818, 752, 717, 694, 607, 568 cm^{-1}. ^{13}C NMR (175 MHz, $CDCl_3$) δ (ppm) = 163.8, 145.8, 139.4, 136.0, 132.2, 129.7, 124.9, 124.2, 122.6, 122.0, 118.6, 114.2, 96.2, 29.8, 24.1. HRMS (EI) m/z: calculated for $C_{40}H_{27}N_3O_2S$, 613.1818; found, 613.1813.

PITT. Under argon atmosphere, [2,2′:5′,2″-terthiophene]-3′,4′-diamine (27.2 mg, 0.097 mmol), 7 mL of anhydrous chloroform, 30 mg (0.061 mmol) of dione **PIDa**, and a catalytic amount of *p*-TSA were heated to 50 °C and left stirring overnight. Then, the solvent was evaporated, and the dark solid was washed with cold and hot methanol to yield 63% (27.9 mg) of a dark blue solid. M.p: >200 °C. ^{1}H NMR (500 MHz, $C_2D_2Cl_4$, 60 °C) δ = 7.94 (bs, 2H), 7.88 (bs, 2H), 7.84 (bs, 2H), 7.67 (bs, 2H), 7.32 (s, 2H), 7.07 (s, 2H), 6.84 (s, 2H), 3.49 (m,

DOI: 10.1021/acs.joc.6b02214
J. Org. Chem. 2016, 81, 11256−11267

2H), 1.97 (bs, 1H), 0.28 (m, 6H). There is a signal at 6.54 ppm that disappears when drops of TFA are added, indicating that this signal may be due to aggregation. FTIR (ATR, CH_2Cl_2): 3069, 2953, 2924, 2858, 1694, 1654, 1581, 1413, 1353, 1319, 1240, 1169, 1134, 1094, 1062, 841, 813, 751, 725, 699, 643, 607 cm^{-1}. HRMS (MALDI-TOF) *m/z*: calculated for $C_{44}H_{32}N_3O_2S_3$ [M + H]+, 730.1651; found, 730.1599 (M +H^+).

NIb. To a solution of 800 mg (3.56 mmol) of acenaphthene anhydride in 160 mL of acetic acid was added dropwise 1.60 mL (7.25 mmol) of the amine and left for 4 days under reflux. Then, water was added until a precipitate appeared. The solid was filtered and throroughly washed with water until the pH turned neutral to obtain 1.25 g (91%) of a clear brown solid. M.p. (dec.): 310 °C. ^{1}H NMR (300 MHz, $CDCl_3$) δ (ppm) = 8.57 (d, 2H, *J* = 7.4 Hz), 7.62(d, 2H, *J* = 7.3 Hz), 7.46 (m, 1H), 7.32 (d, 2H, *J* = 7.7 Hz), 3.62 (s, 4H), 2.74 (m, 2H), 1.15 (d, 12H, *J* = 6.8 Hz). ^{13}C NMR (75 MHz, $CDCl_3$) δ (ppm) = 164.5, 154.3, 146.0, 138.1, 133.4, 131.6, 129.1, 127.3, 124.0, 121.1, 119.4, 31.9, 29.2, 24.1. FTIR (KBr) ν (cm^{-1}) = 3051, 2961, 2925, 2867, 1697, 1659, 1621, 1503, 1456, 1408, 1384, 1362, 1336, 1265, 1234, 1169, 1140, 1096, 1058, 965, 939, 870, 828, 798, 770, 730, 699, 604. HRMS (EI) *m/z*: calculated for $C_{26}H_{25}NO_2$, 383.1885; found, 383.1880.

NIDb. Over a solution of 730 mg (1.9 mmol) of imide **NIb** in chlorobenzene, benzeneseleninic acid anhydride (BSA) (2.2 g, 4.3 mmol) was added. The mixture was heated at 130 °C for 48 h. Then, the solvent was removed, and the solid was dissolved in dichloromethane and washed with water twice. The organic layer was dried with magnesium sulfate, and the solvent was removed by rotary evaporation. The solid was purified by column chromatography (silica gel flash, dichloromethane) to yield 381 mg (50%) of **NIDb** as a yellow solid. M.p. (dec.): 265 °C. ^{1}H NMR (300 MHz, $CDCl_3$) δ (ppm) = 8.88 (d, 2H, *J* = 7.3 Hz), 8.40 (d, 2H, *J* = 7.3 Hz), 7.53 (m, 1H), 7.36 (d, 2H, *J* = 7.7 Hz), 2.71 (m, 2H), 1.16 (d, 12H, *J* = 6.9 Hz). ^{13}C NMR (75 MHz, $CDCl_3$) δ (ppm) = 186.3, 162.8, 145.6, 144.1, 132.8, 132.4, 130.2, 130.1, 127.1, 126.8, 124.4, 123.1, 29.4, 24.1. FTIR (KBr) ν (cm^{-1}) = 2960, 2924, 2853, 1751, 1739, 1712, 1676, 1589, 1452, 1362, 1334, 1259, 1233, 1175, 1136, 1117, 1052, 971, 864, 845, 821, 801, 751, 721. HRMS (EI) *m/z*: calculated for $C_{26}H_{21}NO_4$, 411.1465; found, 411.1463.

NITb. To a degassed solution of naphthalene aromatic dione **NIDb** (30 mg, 0.07 mmol) and 9.0 mg (0.08 mmol) of thiophene-3,4-diamine in 15 mL of $CHCl_3$ was added a catalytic amount of *p*-TSA. The mixture was refluxed overnight under argon. Then, the crude was washed with $NaHCO_3$ and water and dried over anhydrous $MgSO_4$, to give, after chromatography (SiO_2/ dichloromethane/AcOEt (95:0.5)), 15 mg (43%) of a yellow solid. M.p. (dec.): 195 °C. ^{1}H NMR (300 MHz, $CDCl_3$) δ (ppm) = 8.77 (d, 2H, *J* = 7.4 Hz), 8.45(d, 2H, *J* = 7.4 Hz), 8.12 (s, 2H), 7.52 (m, 2H), 7.43 (d, 2H, *J* = 7.7 Hz), 2.78 (m, 2H), 1.18 (d, 12 H, *J* = 6.9 Hz). ^{13}C NMR (75 MHz, $CDCl_3$) δ (ppm) = 163.6, 155.7, 154.0, 145.9, 141.8, 137.2, 136.1, 133.4, 131.1, 130.8, 130.2, 129.8, 129.5, 124.2, 124.1, 121.9, 119.9, 29.3, 24.1. FTIR (KBr) ν (cm^{-1}) = 2963, 2926, 2869, 1800, 1715, 1680, 1645, 1593, 1457, 1383, 1362, 1334, 1235, 1174, 1134, 1100, 1080, 1057, 822, 802, 754. HRMS (EI) *m/z*: calculated for $C_{30}H_{23}N_3O_2S$, 489.1505; found, 489.1507.

■ ASSOCIATED CONTENT

Supporting Information

The Supporting Information is available free of charge on the ACS Publications website at DOI: 10.1021/acs.joc.6b02214.

Copies of NMR spectra, spectroscopic, electrochemical, and computational details (PDF)

■ AUTHOR INFORMATION

Corresponding Authors

*(R.P.O.) E-mail: rocioponce@uma.es.

*(J.L.S.) E-mail: segura@ucm.es.

Notes

The authors declare no competing financial interest.

■ ACKNOWLEDGMENTS

This work was financially supported by MINECO (MAT2014-52305-P and MAT2016-77608-C3-2-P) and the UCM-BSCH joint project (GR3/14-910759). P.E. thanks the URJC for a predoctoral fellowship. Research at University of Malaga was supported by MINECO (CTQ2015-66897-P). R.P.O. and I.A.-M. thank MINECO for a "Ramón y Cajal" research contract and for a predoctoral fellowship, respectively.

■ REFERENCES

(1) Wang, C.; Dong, H.; Hu, W.; Liu, Y.; Zhu, D. *Chem. Rev.* **2012**, *112*, 2208.
(2) Mishra, A.; Bäuerle, P. *Angew. Chem., Int. Ed.* **2012**, *51*, 2020.
(3) Usta, H.; Facchetti, A.; Marks, T. J. *Acc. Chem. Res.* **2011**, *44*, 501.
(4) Kim, F. S.; Ren, G.; Jenekhe, S. A. *Chem. Mater.* **2011**, *23*, 682.
(5) Murphy, A. R.; Fréchet, J. M. J. *Chem. Rev.* **2007**, *107*, 1066.
(6) Allard, S.; Forster, M.; Souharce, B.; Thiem, H.; Scherf, U. *Angew. Chem., Int. Ed.* **2008**, *47*, 4070.
(7) Würthner, F. *Angew. Chem., Int. Ed.* **2001**, *40*, 1037.
(8) Facchetti, A. *Chem. Mater.* **2011**, *23*, 733.
(9) Anthony, J. E.; Facchetti, A.; Heeney, M.; Marder, S. R.; Zhan, X. *Adv. Mater.* **2010**, *22*, 3876.
(10) Wen, Y.; Liu, Y. *Adv. Mater.* **2010**, *22*, 1331.
(11) Newman, C. R.; Frisbie, C. D.; da Silva Filho, D. A.; Brédas, J.-L.; Ewbank, P. C.; Mann, K. R. *Chem. Mater.* **2004**, *16*, 4436.
(12) Tonzola, C. J.; Alam, M. M.; Kaminsky, W.; Jenekhe, S. A. *J. Am. Chem. Soc.* **2003**, *125*, 13548.
(13) Babel, A.; Jenekhe, S. A. *J. Am. Chem. Soc.* **2003**, *125*, 13656.
(14) Zaumseil, J.; Sirringhaus, H. *Chem. Rev.* **2007**, *107*, 1296.
(15) Yan, H.; Chen, Z.; Zheng, Y.; Newman, C.; Quinn, J. R.; Dotz, F.; Kastler, M.; Facchetti, A. *Nature* **2009**, *457*, 679.
(16) Delgado, M. C. R.; Kim, E.-G.; Filho, D. A. d. S.; Bredas, J.-L. *J. Am. Chem. Soc.* **2010**, *132*, 3375.
(17) Dong, H.; Fu, X.; Liu, J.; Wang, Z.; Hu, W. *Adv. Mater.* **2013**, *25*, 6158.
(18) Reghu, R. R.; Bisoyi, H. K.; Grazulevicius, J. V.; Anjukandi, P.; Gaidelis, V.; Jankauskas, V. *J. Mater. Chem.* **2011**, *21*, 7811.
(19) Wurthner, F.; Stolte, M. *Chem. Commun.* **2011**, *47*, 5109.
(20) Singh, T. B.; Erten, S.; Günes, S.; Zafer, C.; Turkmen, G.; Kuban, B.; Teoman, Y.; Sariciftci, N. S.; Icli, S. *Org. Electron.* **2006**, *7*, 480.
(21) Ventura, B.; Langhals, H.; Bock, B.; Flamigni, L. *Chem. Commun.* **2012**, *48*, 4226.
(22) Damaceanu, M.-D.; Constantin, C.-P.; Bruma, M.; Pinteala, M. *Dyes Pigm.* **2013**, *99*, 228.
(23) Lucenti, E.; Botta, C.; Cariati, E.; Righetto, S.; Scarpellini, M.; Tordin, E.; Ugo, R. *Dyes Pigm.* **2013**, *96*, 748.
(24) Kozma, E.; Kotowski, D.; Catellani, M.; Luzzati, S.; Famulari, A.; Bertini, F. *Dyes Pigm.* **2013**, *99*, 329.
(25) Shibano, Y.; Umeyama, T.; Matano, Y.; Imahori, H. *Org. Lett.* **2007**, *9*, 1971.
(26) Choi, H.; Paek, S.; Song, J.; Kim, C.; Cho, N.; Ko, J. *Chem. Commun.* **2011**, *47*, 5509.
(27) Huang, C.; Barlow, S.; Marder, S. R. *J. Org. Chem.* **2011**, *76*, 2386.
(28) Hwang, Y.-J.; Earmme, T.; Courtright, B. A. E.; Eberle, F. N.; Jenekhe, S. A. *J. Am. Chem. Soc.* **2015**, *137*, 4424.
(29) Jackson, N. E.; Savoie, B. M.; Marks, T. J.; Chen, L. X.; Ratner, M. A. *J. Phys. Chem. Lett.* **2015**, *6*, 77.
(30) Shukla, D.; Nelson, S. F.; Freeman, D. C.; Rajeswaran, M.; Ahearn, W. G.; Meyer, D. M.; Carey, J. T. *Chem. Mater.* **2008**, *20*, 7486.
(31) Zhan, X.; Facchetti, A.; Barlow, S.; Marks, T. J.; Ratner, M. A.; Wasielewski, M. R.; Marder, S. R. *Adv. Mater.* **2011**, *23*, 268.
(32) Guo, X.; Facchetti, A.; Marks, T. J. *Chem. Rev.* **2014**, *114*, 8943.
(33) Gsänger, M.; Bialas, D.; Huang, L.; Stolte, M.; Würthner, F. *Adv. Mater.* **2016**, *28*, 3615.

DOI: 10.1021/acs.joc.6b02214
J. Org. Chem. 2016, 81, 11256−11267

(34) Lee, W.-Y.; Oh, J. H.; Suraru, S.-L.; Chen, W.-C.; Würthner, F.; Bao, Z. *Adv. Funct. Mater.* **2011**, *21*, 4173.
(35) Oh, J. H.; Suraru, S. L.; Lee, W.-Y.; Könemann, M.; Höffken, H. W.; Röger, C.; Schmidt, R.; Chung, Y.; Chen, W.-C.; Würthner, F.; Bao, Z. *Adv. Funct. Mater.* **2010**, *20*, 2148.
(36) Jones, B. A.; Facchetti, A.; Marks, T. J.; Wasielewski, M. R. *Chem. Mater.* **2007**, *19*, 2703.
(37) Jones, B. A.; Facchetti, A.; Wasielewski, M. R.; Marks, T. J. *J. Am. Chem. Soc.* **2007**, *129*, 15259.
(38) He, T.; Stolte, M.; Würthner, F. *Adv. Mater.* **2013**, *25*, 6951.
(39) He, T.; Stolte, M.; Burschka, C.; Hansen, N. H.; Musiol, T.; Kälblein, D.; Pflaum, J.; Tao, X.; Brill, J.; Würthner, F. *Nat. Commun.* **2015**, *6*.
(40) Malenfant, P. R. L.; Dimitrakopoulos, C. D.; Gelorme, J. D.; Kosbar, L. L.; Graham, T. O.; Curioni, A.; Andreoni, W. *Appl. Phys. Lett.* **2002**, *80*, 2517.
(41) Tatemichi, S.; Ichikawa, M.; Koyama, T.; Taniguchi, Y. *Appl. Phys. Lett.* **2006**, *89*, 112108.
(42) Schmidt, R.; Oh, J. H.; Sun, Y.-S.; Deppisch, M.; Krause, A.-M.; Radacki, K.; Braunschweig, H.; Könemann, M.; Erk, P.; Bao, Z.; Würthner, F. *J. Am. Chem. Soc.* **2009**, *131*, 6215.
(43) Schmidt, R.; Ling, M. M.; Oh, J. H.; Winkler, M.; Könemann, M.; Bao, Z.; Würthner, F. *Adv. Mater.* **2007**, *19*, 3692.
(44) Jones, B. A.; Ahrens, M. J.; Yoon, M.-H.; Facchetti, A.; Marks, T. J.; Wasielewski, M. R. *Angew. Chem., Int. Ed.* **2004**, *43*, 6363.
(45) Jones, B. A.; Facchetti, A.; Wasielewski, M. R.; Marks, T. J. *Adv. Funct. Mater.* **2008**, *18*, 1329.
(46) Ortiz, R. P.; Herrera, H.; Blanco, R.; Huang, H.; Facchetti, A.; Marks, T. J.; Zheng, Y.; Segura, J. L. *J. Am. Chem. Soc.* **2010**, *132*, 8440.
(47) Ortiz, R. P.; Herrera, H.; Seoane, C.; Segura, J. L.; Facchetti, A.; Marks, T. J. *Chem. - Eur. J.* **2012**, *18*, 532.
(48) Gsänger, M.; Oh, J. H.; Könemann, M.; Höffken, H. W.; Krause, A.-M.; Bao, Z.; Würthner, F. *Angew. Chem., Int. Ed.* **2010**, *49*, 740.
(49) Ponce Ortiz, R.; Herrera, H.; Mancheño, M. J.; Seoane, C.; Segura, J. L.; Mayorga Burrezo, P.; Casado, J.; López Navarrete, J. T.; Facchetti, A.; Marks, T. J. *Chem. - Eur. J.* **2013**, *19*, 12458.
(50) Herrera, H.; de Echegaray, P.; Urdanpilleta, M.; Mancheno, M. J.; Mena-Osteritz, E.; Bauerle, P.; Segura, J. L. *Chem. Commun.* **2013**, *49*, 713.
(51) Li, H.; Kim, F. S.; Ren, G.; Hollenbeck, E. C.; Subramaniyan, S.; Jenekhe, S. A. *Angew. Chem., Int. Ed.* **2013**, *52*, 5513.
(52) Li, H.; Kim, F. S.; Ren, G.; Jenekhe, S. A. *J. Am. Chem. Soc.* **2013**, *135*, 14920.
(53) Kaiser, T. E.; Wang, H.; Stepanenko, V.; Würthner, F. *Angew. Chem., Int. Ed.* **2007**, *46*, 5541.
(54) Endres, A. H.; Schaffroth, M.; Paulus, F.; Reiss, H.; Wadepohl, H.; Rominger, F.; Krämer, R.; Bunz, U. H. F. *J. Am. Chem. Soc.* **2016**, *138*, 1792.
(55) Alaei, P.; Rouhani, S.; Gharanjig, K.; Ghasemi, J. *Spectrochim. Acta, Part A* **2012**, *90*, 85.
(56) Mee, S. P. H.; Lee, V.; Baldwin, J. E. *Chem. - Eur. J.* **2005**, *11*, 3294.
(57) Mee, S. P. H.; Lee, V.; Baldwin, J. E. *Angew. Chem., Int. Ed.* **2004**, *43*, 1132.
(58) Avlasevich, Y.; Li, C.; Mullen, K. *J. Mater. Chem.* **2010**, *20*, 3814.
(59) Sakamoto, T.; Pac, C. *J. Org. Chem.* **2001**, *66*, 94.
(60) Oh, J. H.; Lee, W.-Y.; Noe, T.; Chen, W.-C.; Könemann, M.; Bao, Z. *J. Am. Chem. Soc.* **2011**, *133*, 4204.
(61) Sanguineti, A.; Sassi, M.; Turrisi, R.; Ruffo, R.; Vaccaro, G.; Meinardi, F.; Beverina, L. *Chem. Commun.* **2013**, *49*, 1618.
(62) Marom, H.; Popowski, Y.; Antonov, S.; Gozin, M. *Org. Lett.* **2011**, *13*, 5532.
(63) Scholl, R.; Mansfeld, J. *Ber. Dtsch. Chem. Ges.* **1910**, *43*, 1734.
(64) Kovacic, P.; Jones, M. B. *Chem. Rev.* **1987**, *87*, 357.
(65) Berresheim, A. J.; Müller, M.; Müllen, K. *Chem. Rev.* **1999**, *99*, 1747.
(66) Watson, M. D.; Fechtenkötter, A.; Müllen, K. *Chem. Rev.* **2001**, *101*, 1267.
(67) King, B. T.; Kroulík, J.; Robertson, C. R.; Rempala, P.; Hilton, C. L.; Korinek, J. D.; Gortari, L. M. *J. Org. Chem.* **2007**, *72*, 2279.
(68) Iyer, V. S.; Yoshimura, K.; Enkelmann, V.; Epsch, R.; Rabe, J. P.; Müllen, K. *Angew. Chem., Int. Ed.* **1998**, *37*, 2696.
(69) Dötz, F.; Brand, J. D.; Ito, S.; Gherghel, L.; Müllen, K. *J. Am. Chem. Soc.* **2000**, *122*, 7707.
(70) Wang, Z.; Dötz, F.; Enkelmann, V.; Müllen, K. *Angew. Chem., Int. Ed.* **2005**, *44*, 1247.
(71) Wu, J.; Grimsdale, A. C.; Mullen, K. *J. Mater. Chem.* **2005**, *15*, 41.
(72) Boden, N.; Bushby, R. J.; Cammidge, A. N.; Duckworth, S.; Headdock, G. *J. Mater. Chem.* **1997**, *7*, 601.
(73) Boden, N.; Bushby, R. J.; Headdock, G.; Lozman, O. R.; Wood, A. *Liq. Cryst.* **2001**, *28*, 139.
(74) Simpson, C. D.; Mattersteig, G.; Martin, K.; Gherghel, L.; Bauer, R. E.; Räder, H. J.; Müllen, K. *J. Am. Chem. Soc.* **2004**, *126*, 3139.
(75) Kubel, C.; Eckhardt, K.; Enkelmann, V.; Wegner, G.; Mullen, K. *J. Mater. Chem.* **2000**, *10*, 879.
(76) Zhai, L.; Shukla, R.; Rathore, R. *Org. Lett.* **2009**, *11*, 3474.
(77) Zhang, L.; Lo, K. C.; Chan, W. K. *Chem. Commun.* **2014**, *50*, 4245.
(78) Takeda, Y.; Andrew, T. L.; Lobez, J. M.; Mork, A. J.; Swager, T. M. *Angew. Chem., Int. Ed.* **2012**, *51*, 9042.
(79) Mateo-Alonso, A. *Chem. Soc. Rev.* **2014**, *43*, 6311.
(80) Malagoli, M.; Brédas, J. L. *Chem. Phys. Lett.* **2000**, *327*, 13.
(81) Shao, C.; Grune, M.; Stolte, M.; Wurthner, F. *Chem. - Eur. J.* **2012**, *18*, 13665.
(82) Walter, S. R.; Youn, J.; Emery, J. D.; Kewalramani, S.; Hennek, J. W.; Bedzyk, M. J.; Facchetti, A.; Marks, T. J.; Geiger, F. M. *J. Am. Chem. Soc.* **2012**, *134*, 11726.
(83) Oliva, M. M.; Pappenfus, T. M.; Melby, J. H.; Schwaderer, K. M.; Johnson, J. C.; McGee, K. A.; da Silva Filho, D. A.; Bredas, J.-L.; Casado, J.; López Navarrete, J. T. *Chem. - Eur. J.* **2010**, *16*, 6866.
(84) Kenning, D. D.; Mitchell, K. A.; Calhoun, T. R.; Funfar, M. R.; Sattler, D. J.; Rasmussen, S. C. *J. Org. Chem.* **2002**, *67*, 9073.
(85) Gudeika, D.; Lygaitis, R.; Mimaitė, V.; Grazulevicius, J. V.; Jankauskas, V.; Lapkowski, M.; Data, P. *Dyes Pigm.* **2011**, *91*, 13.
(86) Kitamura, C.; Tanaka, S.; Yamashita, Y. *Chem. Mater.* **1996**, *8*, 570.
(87) Frisch, M. J.; Trucks, G. W.; Schlegel, H. B.; Scuseria, G. E.; Robb, M. A.; Cheeseman, J. R.; Scalmani, G.; Barone, V.; Mennucci, B.; Petersson, G. A.; Nakatsuji, H.; Caricato, M.; Li, X.; Hratchian, H. P.; Izmaylov, A. F.; Bloino, J.; Zheng, G.; Sonnenberg, J. L.; Hada, M.; Ehara, M.; Toyota, K.; Fukuda, R.; Hasegawa, J.; Ishida, M.; Nakajima, T.; Honda, Y.; Kitao, O.; Nakai, H.; Vreven, T.; Montgomery, J. A., Jr.; Peralta, J. E.; Ogliaro, F.; Bearpark, M. J.; Heyd, J.; Brothers, E. N.; Kudin, K. N.; Staroverov, V. N.; Kobayashi, R.; Normand, J.; Raghavachari, K.; Rendell, A. P.; Burant, J. C.; Iyengar, S. S.; Tomasi, J.; Cossi, M.; Rega, N.; Millam, N. J.; Klene, M.; Knox, J. E.; Cross, J. B.; Bakken, V.; Adamo, C.; Jaramillo, J.; Gomperts, R.; Stratmann, R. E.; Yazyev, O.; Austin, A. J.; Cammi, R.; Pomelli, C.; Ochterski, J. W.; Martin, R. L.; Morokuma, K.; Zakrzewski, V. G.; Voth, G. A.; Salvador, P.; Dannenberg, J. J.; Dapprich, S.; Daniels, A. D.; Farkas, Ö.; Foresman, J. B.; Ortiz, J. V.; Cioslowski, J.; Fox, D. J. *Gaussian 09*, rev. B.01; Gaussian, Inc.: Wallingford, CT, 2009.

DOI: 10.1021/acs.joc.6b02214
J. Org. Chem. 2016, 81, 11256−11267